ELSEVIER

Journal of Nuclear Materials 318 (2003) 143–150

journal of nuclear materials

www.elsevier.com/locate/jnucmat

Influence of PbBi environment on the low-cycle fatigue behavior of SNS target container materials

D. Kalkhof, M. Grosse *

Paul Scherrer Institut, Nuclear Energy and Safety Department, CH- 5232 Villigen PSI, Switzerland

Abstract

The low-cycle fatigue (LCF) behavior of the stainless steel 316L and the 10.5Cr-steel Manet-II was investigated at 260 °C in air and in stagnant lead–bismuth (PbBi). At low-strain levels, the fatigue lives for 316L in PbBi and air were comparable. At total strain amplitudes of 0.50% and higher a weak influence of PbBi was observed. In contrast to 316L, the results of LCF tests for Manet-II in PbBi showed a significant reduction of lifetime for all applied strain amplitudes. In the worst case the cycle number to crack initiation was reduced by a factor of ≈ 7 compared with the comparable test in air. For the low-strain amplitude of 0.30%, fatigue tests conducted at a frequency of 0.1 Hz had shorter fatigue lives than at a frequency of 1.0 Hz. For Manet-II the crack propagation in PbBi was much faster than in air, and failure immediate followed the formation of the first macroscopic crack.

1. Introduction

In contrast to other existing and planned spallation neutron sources, like ISIS (GB), ESS (EU) or SNS (USA), SINQ (CH) at the Paul Scherrer Institute does not produce a pulsed but a constant intensity neutron beam. However, due to beam trips cyclic loading is an important design consideration for the SINQ-targets. The Fig. 1(a) and (b) show the beam history during normal service and service with operational problems. Under normal service conditions between 30 and 50 beam trips per day are usual. If operational problems occur, the number of beam trips can increase to more than 200. Consequently, beam trips in the order of magnitude of 10^4 are expected for the design lifetime of the planned SINQ target-window.

The design of the planned SINQ liquid metal target is described by Bauer [1]. In a liquid metal target the target material is used as the primary cooling loop. It must, therefore, not only perform well as a spallation target but must also have suitable properties to be moved around in a loop. The great advantages of the lead–bismuth eutectic mixture are its low melting point of only 125 °C and the fact that it does not changes its volume upon solidification. In choosing a structural material to contain a liquid metal target several factors must be taken into account:

- behavior under irradiation in a spectrum typical for spallation sources,
- resistance to liquid metal corrosion and embrittlement,
- resistance to fatigue (LCF, HCF) in a liquid metal environment,
- neutronic properties (absorption).

Candidate target-container materials include austenitic stainless steels like AISI 316L and ferritic–martensitic steels like Manet-II. Design of the target-window has to ensure that the cyclic load applied to the window is much lower than the critical load, which leads to crack initiation after 10^4 load cycles. LCF tests at 260 °C in air indicated that this critical load corresponds to a total strain amplitude of about 0.3% for Manet-II which is much higher than the design strain amplitude of 0.03%

* Corresponding author. Tel.: +41-56 310 2113; fax: +41-56 310 2199.

E-mail address: micro.grosse@psi.ch (M. Grosse).

0022-3115/03/$ - see front matter
doi:10.1016/S0022-3115(03)00015-1

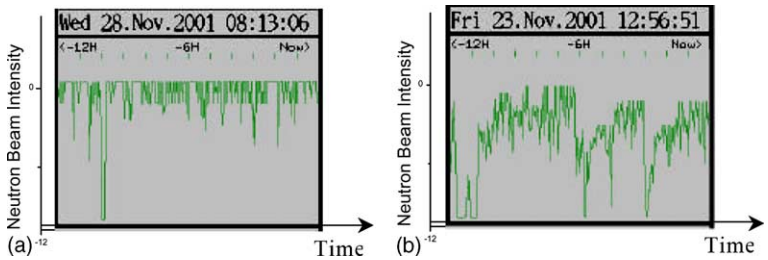

Fig. 1. Beam intensity vs. operational time (a) for normal service (b) for service with operational problems.

for the SINQ target-window. However, LCF tests in PbBi environment are necessary to determine the influence of PbBi on this critical load value.

Austenitic stainless steels have been widely used in the nuclear industry, because of their excellent ductility, corrosion resistance and irradiation performance. Recently, 316LN (low carbon, nitrogen-containing) stainless steel was selected as a container material for the mercury target of the SNS at the Oak Ridge National Laboratory [2]. The influence of mercury environment on the fatigue behavior of 316LN steel at stress amplitudes above the endurance limit mercury was deleterious to fatigue life [3]. This trend was believed to result from liquid metal embrittlement in mercury. As stress amplitude decreased fatigue lives in mercury and air converged on a common endurance limit.

Compared with austenitic stainless steels, the higher initial yield strength, low thermal expansion coefficient and good thermal conductivity of ferritic–martensitic steels greatly reduce concerns about fatigue damage produced by thermal transients in this material. A comprehensive survey about the cyclic stress–strain-time response of 9Cr–1Mo–V–Nb steels at temperatures from 25 to 600 °C was given by Swindeman [4]. Research on the applicability of 9Cr-steels to the steam generator of the demonstration fast breeder reactor was performed by a committee of the Japan Welding Engineering Society. In that program, exploratory tests, which included tensile, LCF, and creep tests, were conducted on different 9Cr–1Mo, 9Cr–1Mo–V–Nb, and 9Cr–2Mo steels and their weldments. The summary of results obtained in this study were presented by Asada et al. [5]. Whereas the fatigue behavior of the ferritic–martensitic steels in air is well known, there is a lack of knowledge about the fatigue behavior in a liquid metal environment. The aim of this work was to investigate the influence of the liquid PbBi environment on the LCF behavior of 316L stainless steel and the 10.5Cr-steel Manet-II.

2. Experimental procedures

Fully reversed ($R = -1$) strain controlled LCF tests were performed on a servo-hydraulic Schenck machine with a load capacity of 250 kN. The test machine was controlled by the Instron FastTrack 8800 control unit delivered by the Instron Corporation, USA. For the strain measurement a clip gage EXA 40-1.25 of the Sandner Messtechnik Company, Germany, was applied. It allows strain measurements up to a temperature of 300 °C without any cooling. The gage length was 40 mm. In all tests the specimens were heated in a special climatic chamber Instron SFL EC65, made by the Company SFL, UK. The climatic chamber was adopted to the LCF test grips. To keep the specimen temperature constant, the surface temperature was continuously measured whereas the ambient temperature was controlled. For the loading frequency of 1.0 Hz and the total strain amplitude of 0.40% without any cooling or heating the temperature measured at the surface of 316L was 80 °C. To obtain results for room temperature, the specimens were cooled with a ventilator.

LCF tests were conducted at total strain amplitudes from 0.2% to 1.0%. Generally, the test frequency was 1.0 Hz. A few tests with a total strain amplitude of 0.3% were performed at a frequency of 0.1 Hz. In order to define macroscopic crack initiation the generally

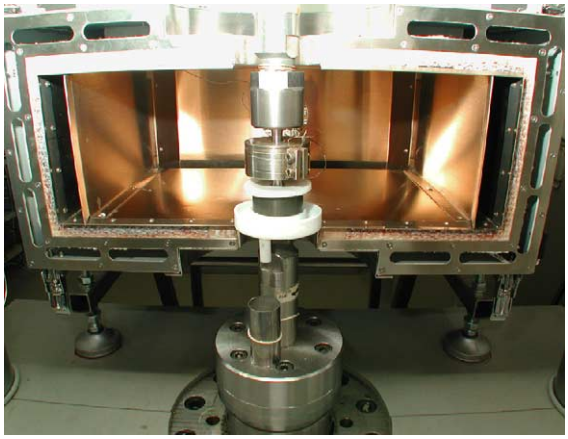

Fig. 2. View of the LCF grips, climatic chamber and PbBi container. The LCF grips were mounted to a 250 kN servo-hydraulic Schenck machine. A specially designed container was employed for LCF tests in PbBi.

Table 1
Chemical composition in weight percent of 316L and Manet-II

	C	Cr	Ni	Ti	Si	Mn	P	S	Mo	Co
316L	0.020	17.20	12.60	0.003	0.370	1.67	0.024	0.003	2.60	0.350
Manet-II	0.080	10.50	0.644	0.001	0.263	0.927	0.007	0.005	0.550	0.006

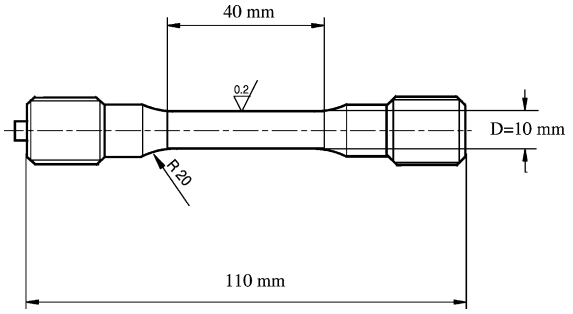

Fig. 3. Dimensions of LCF specimen. The specimens were fabricated utilizing low-stress grinding and polishing.

accepted criteria of 5% load drop in the stress amplitude was applied. LCF tests were stopped when the 5% load drop was reached and the cycle number for crack initiation was recorded. In order to conduct LCF tests in the PbBi environment, a container made from 304 stainless steel was used (Fig. 2). The gage section of the specimen was immersed in PbBi enclosed in the container. The container was attached to the specimen with a silicon-rubber sealant, which could be removed from the specimen after the test. During fatigue tests, the gage section of the specimens remained in contact with the PbBi in the container. Tests were performed at room temperature and 260 °C in air and at 260 °C in stagnant liquid PbBi.

Specimens were tested in the as-received state with no additional thermal treatments prior to testing. The materials were analyzed by means of Inductive Coupled Plasma Emission Photometry (ICP-OES) within an uncertainty of 2% of the measured value. The chemical compositions of the investigated materials 316L and Manet-II are shown in Table 1. The geometry of the cylindrical-bar specimen used is illustrated in Fig. 3. The LCF specimen has a total length of 110 mm, a gage length of 40 mm and a gage diameter of 10 mm. Specimen fabrication employed turning, low-stress grinding and mechanically polishing operations.

3. Results and discussion

3.1. Low-cycle fatigue tests in air

Fatigue experiments were conducted at different total strain amplitudes. In Figs. 4 and 5, the typical stress amplitude vs. cycle number curves for 316L and Manet-II in air at 260 °C are shown. The material behavior was characterized by a hardening in the first 10 cycles followed by softening out to the crack initiation. The LCF curves exhibited a very small scatter for all strain amplitudes. The 5% load drop criteria for determining the cycle number representing macroscopic crack initiation yielded reproducible results. Only for the total strain amplitude of 0.30% did some scatter occur. In Fig. 6, test results for the LCF behavior in air are summarized. The applied strain vs. cycles to crack initiation curves for 316L and Manet-II showed a very small scatter at room temperature and at 260 °C. The 316L stainless steel exhibited a slight reduction in the cycle number for crack initiation at 260 °C compared with room

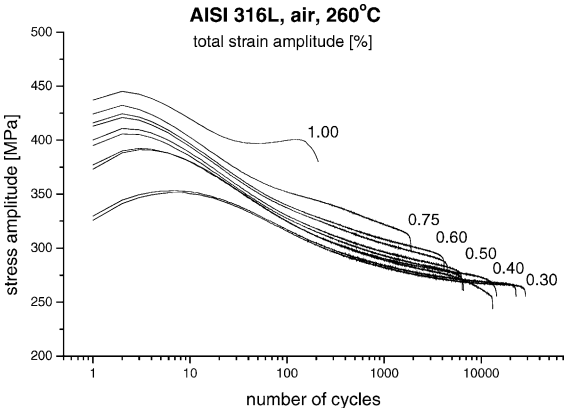

Fig. 4. Stress amplitude vs. cycle number curves for 316L stainless steel at 260 °C in air.

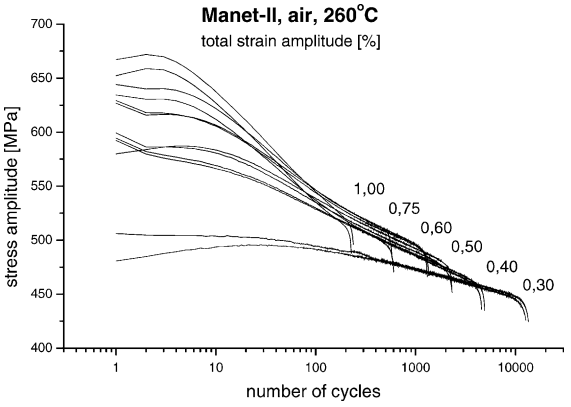

Fig. 5. Stress amplitude vs. cycle number curves for Manet-II at 260 °C in air.

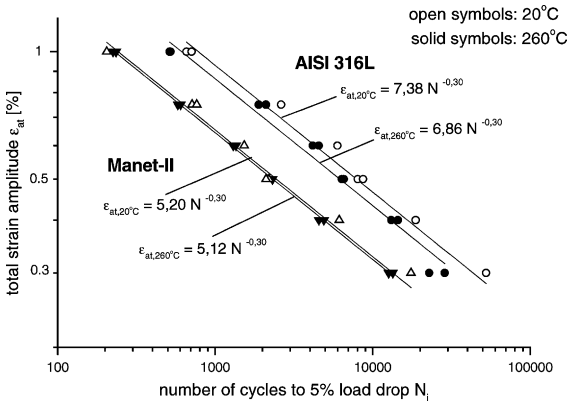

Fig. 6. Total strain amplitude vs. cycle number for crack initiation curves of 316L stainless steel and Manet-II in air at room temperature and 260 °C.

temperature. On the other hand, Manet-II showed no temperature dependency. Generally, cycle life for 316L stainless steel was longer than for Manet-II. For the total strain amplitude of 0.30% at 260 °C, the mean value of the cycle number for crack initiation was 25 780 for 316L compared with 13 280 for Manet-II. The LCF data were analyzed according to the Coffin–Manson-law:

$$\Delta\varepsilon_{\text{plastic}} N_c^a = \text{const.} \tag{1}$$

$\Delta\varepsilon_{\text{plastic}}$ is the plastic strain amplitude, and a is the Coffin–Manson exponent. For both materials an exponent of 0.30 was obtained for fatigue tests in air.

3.2. Low-cycle fatigue tests in PbBi

The influence of the PbBi environment on the LCF behavior is illustrated in Figs. 7 and 8. Fig. 7 shows the stress amplitude vs. cycle number curves for 316L stainless steel at 260 °C in air and in liquid PbBi tested

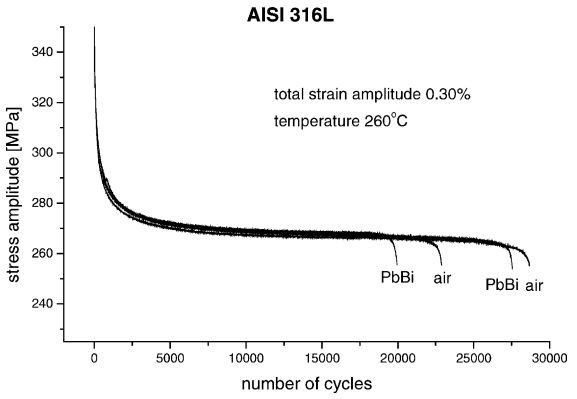

Fig. 7. Stress amplitude vs. cycle number at the total strain amplitude of 0.30% in air and PbBi for 316L stainless steel.

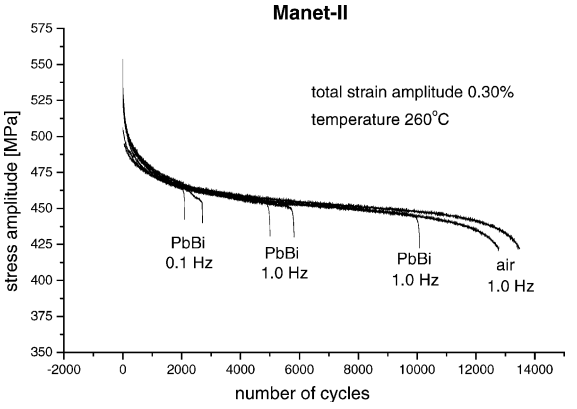

Fig. 8. Stress amplitude vs. cycle number at the total strain amplitude of 0.30% in air and PbBi for Manet-II.

with a total strain amplitude of 0.30%. For 316L at the low-strain level of 0.30% some scatter of fatigue lives was observed in both air and liquid PbBi environment. Cycle life was only slightly reduced from 25 780 cycles in air to 23 780 cycles in PbBi (mean values). In contrast to 316L the cycle lives of Manet-II were significantly reduced in the PbBi environment. This strong influence of PbBi on the fatigue behavior of Manet-II is shown in Fig. 8. The mean value of the cycle number to crack initiation at the strain amplitude of 0.30% was reduced from 13 280 cycles in air to 6980 cycles in PbBi at a test frequency of 1.0 Hz. Furthermore, cycle life was reduced with a decrease in test frequency. At 0.1 Hz the mean value of the cycle number to crack initiation was 2410 cycles. A large scatter for the cycle numbers representing crack initiation was observed for Manet-II in PbBi.

In Figs. 9 and 10, the behavior of plastic strain amplitude in the tension phase of the cyclic loading is shown as a function of the cycle number. The plastic

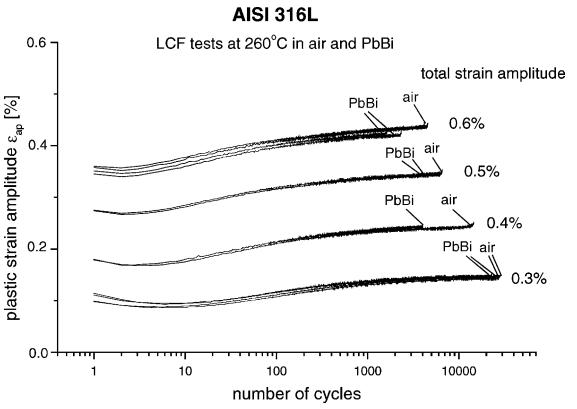

Fig. 9. Behavior of the plastic strain amplitude in the tension phase of cyclic loading as a function of the cycle number for 316L stainless steel at different total strain amplitudes in air and PbBi.

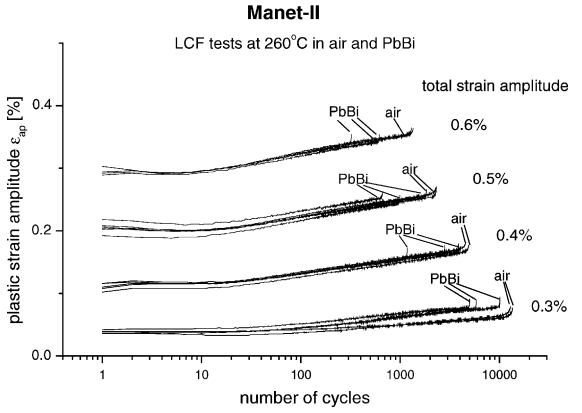

Fig. 10. Behavior of the plastic strain amplitudes in the tension phase of cyclic loading as a function of the cycle number for Manet-II at different total strain amplitudes in air and in PbBi.

strain amplitudes for a total strain amplitude of 0.30% were relatively low (0.10% for 316L and 0.05% for Manet-II). As mentioned above the predominant behavior is softening, excluding the first 10 cycles. For both materials, the degree of softening did not depend on the environment.

3.3. Low-cycle fatigue crack growth in PbBi

During the LCF tests for Manet-II in PbBi it was surprising that just as the 5% load drop was reached the servo-hydraulic machine abruptly stopped the test. The reason is illustrated in Fig. 12. The Figs. 11 and 12 magnify the LCF behavior in the region of near the end of tests conducted at the total strain amplitude of 0.30%. For 316L stainless steel, the crack propagation was slightly faster in PbBi than in air (Fig. 11). In Fig. 12, the crack propagation for Manet-II under the PbBi influence was very fast compared with the crack growth in air. This fast crack propagation could be caused by the

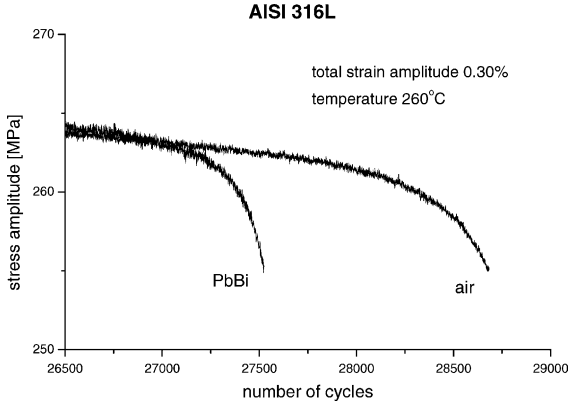

Fig. 11. Crack propagation range for 316L stainless steel.

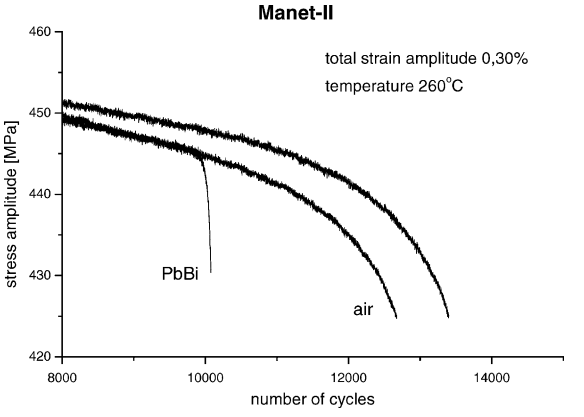

Fig. 12. Crack propagation range for Manet-II.

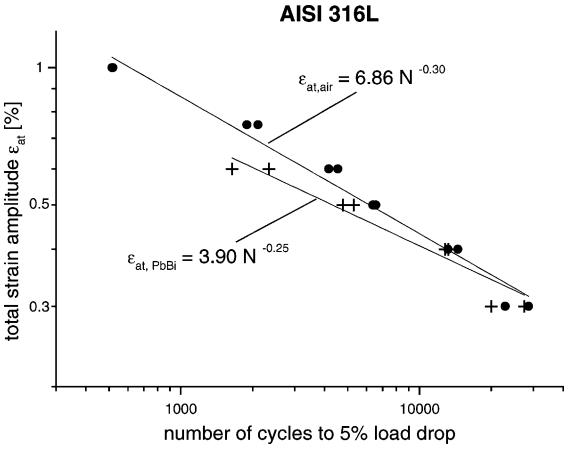

Fig. 13. Total strain amplitude vs. cycle number for crack initiation curves for 316L stainless steel in air and PbBi at 260 °C.

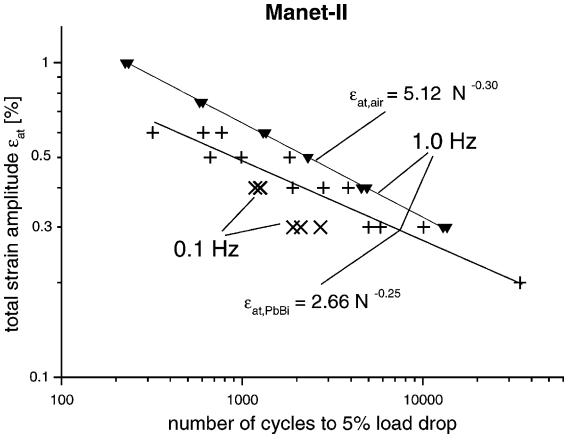

Fig. 14. Total strain amplitude vs. cycle number for crack initiation curves for Manet-II in air and PbBi at 260 °C.

wedge effect that has been observed in other liquid metal fatigue investigations [6]. From high temperature experiments in air and sodium it can be derived that heavy oxidation in cracks leads to crack tip blunting and consequently to a lowering of the crack growth rate. On the other hand, depending on the degree of wetting, the wetting within the running crack leads to an addition to the tensile stress during crack closure, which does not result in crack tip blunting. The sharp crack remains and this seems to be the reason for the observed fast crack growth of Manet-II in PbBi.

3.4. Effect of PbBi

Figs. 13 and 14, give the LCF test results in air and stagnant PbBi environment for 316L and Manet-II, respectively. As shown in Fig. 13, the fatigue lives for 316L at lower total strain amplitudes in PbBi appeared to be similar in comparison with the results in air. At high strain amplitudes of 0.50% and 0.60%, there was a little influence of the PbBi environment on the cycle number to crack initiation. In comparison the influence of PbBi on the fatigue behavior of Manet-II was very strong.

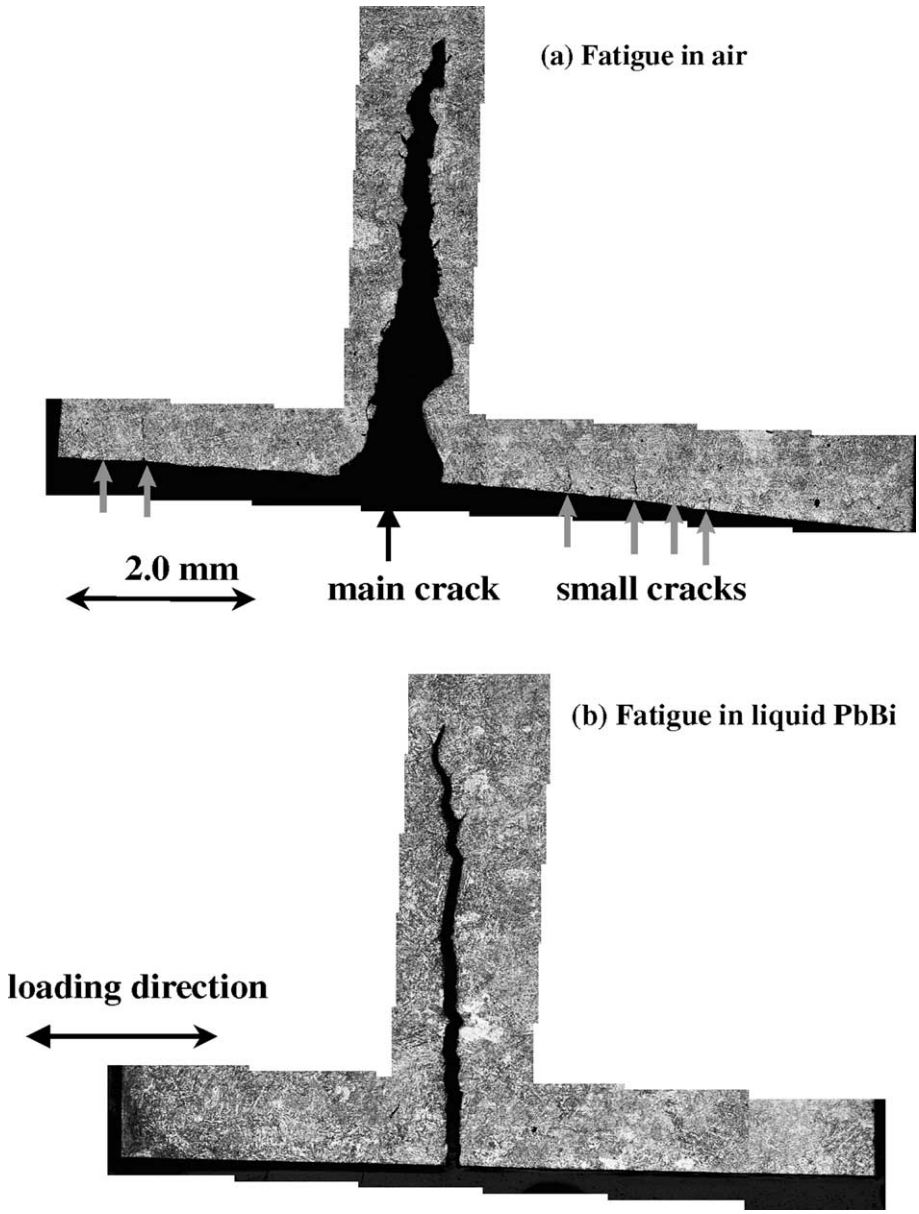

Fig. 15. Photomicrographs of specimens tested in (a) air and (b) in PbBi. Arrows mark the microcrack positions.

Fig. 14 illustrates that there was a large scatter in the cycle number to crack initiation in PbBi. In the worst case (total strain amplitude 0.30%, frequency 0.1 Hz) the cycle life for Manet-II in PbBi was reduced by a factor of ≈7. Although the scatter was large, the data were analysed according to the Coffin–Manson law. For both materials, the Coffin–Manson exponent in PbBi was 0.25 compared with 0.30 in air. This lower exponent indicated different fatigue fracture mechanisms in air and PbBi. Refering to Fig. 10 the critical load strain level for a 10^4 cycle life has not yet been determined. Additional testing at total strain amplitudes less than 0.30% would be necessary.

3.5. Post-test microstructure

Following fatigue tests, a light microscope and a scanning-electron microscope (SEM) were used to observe the crack surfaces of the Manet-II specimens. LCF specimens were cut parallel to the longitudinal axis. The Fig. 15(a) and (b) compare specimens tested in air and PbBi. The crack initiation mechanisms in air and PbBi were different. In air, a main crack and a number of small cracks starting at the specimen surface were found. A view of the surface of a Manet-II specimen fatigued in air is shown in Fig. 16. In PbBi, only a single crack was observed. In Fig. 17, the SEM secondary electron image

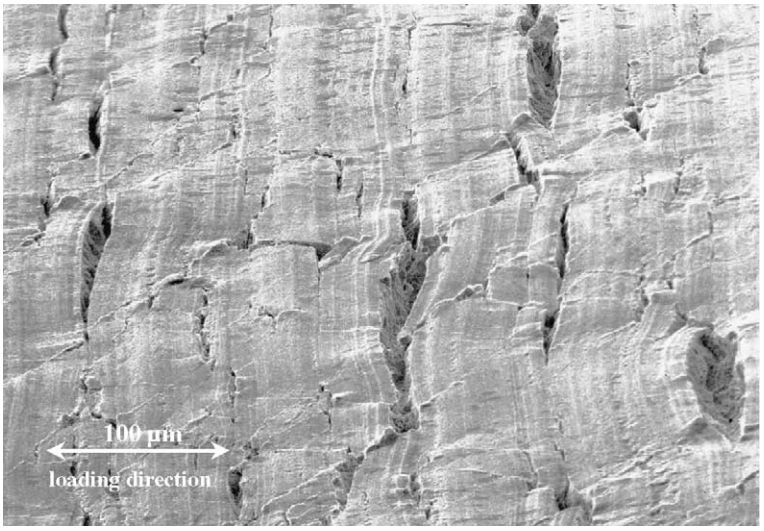

Fig. 16. View (SEM) of the surface of a Manet-II specimen fatigued in air. Many small cracks at the surface were found.

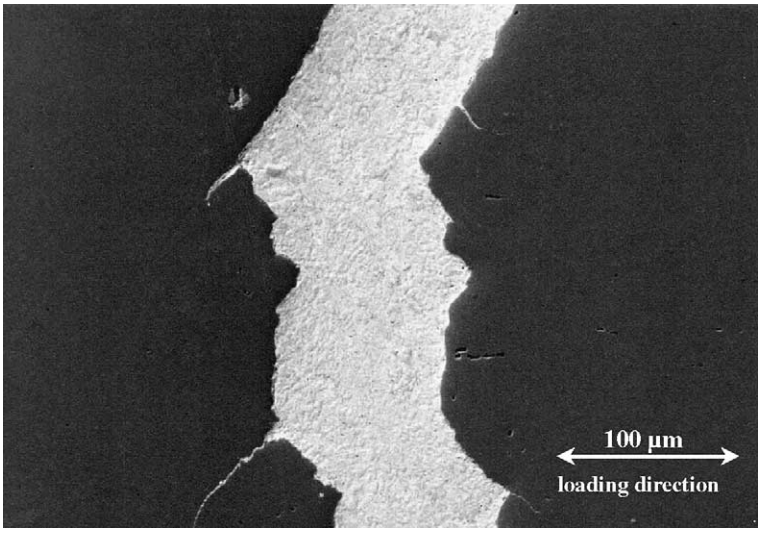

Fig. 17. Secondary electron image of the main crack and sub-cracks of a Manet-II specimen. The PbBi penetrated into the smallest sub-cracks.

showed that liquid PbBi penetrated into even the smallest sub-cracks. Rapid crack propagation was the result of this penetration.

4. Summary

The present study investigated the influence of the PbBi environment on the fatigue lives of 316L stainless steel and Manet-II. The environmental effect depended on both the applied strain and test frequency. At low-strain amplitudes, the fatigue lives for 316L in air and PbBi were comparable. At total strain amplitudes of 0.50% and higher, a weak influence was observed. It is thought that the good fatigue resistance in PbBi is caused by the formation of stable protective oxide layers on the surface of the 316L stainless steel. On the other hand, the LCF results for Manet-II showed a strong reduction in cycle life for a given load amplitude in PbBi compared with air. The crack propagation in PbBi was much faster and the formation of a single crack led to failure of the LCF specimen. Fatigue tests conducted at the low frequency of 0.1 Hz resulted in shorter fatigue lives for a total strain amplitude of 0.30%. This frequency effect is believed to result from liquid metal embrittlement in PbBi.

This study focused on LCF testing at total strain amplitudes characterized by plastic deformation. Additional testing at lower strain amplitudes, particularly in PbBi would be needed to achieve 10^4 cycles, corresponding to the service period of the planned SINQ liquid metal target-window. Consequently, plastic strains especially at local stress concentrations (notches, rough surfaces, welds and edges) have to be excluded under all possible service conditions for the SINQ target-window. It appears that longer lasting fatigue testing performed in the elastic strain range may be needed to find the stress amplitude limit for the expected service cycle number (10^4).

5. Conclusions

1. After an initial hardening, the 316L stainless steel and the Manet-II softened under LCF conditions. For both materials, the extent of softening did not change in PbBi compared with air.
2. Whereas the influence of the PbBi environment on the LCF behavior of 316L was weak, the fatigue lives for Manet-II were significantly reduced for all applied strains. In the worst case, the fatigue life in PbBi was reduced by a factor of ≈ 7, compared with air.
3. The exponent in the Coffin–Manson law relating the cyclic life to inelastic strain range was dependent on the environment. The exponent for LCF tests in air was 0.30 for both materials. However, in PbBi the exponent was slightly reduced to 0.25. This trend indicated that the fatigue fracture mechanisms were different in air and PbBi.
4. For Manet-II, very fast fatigue crack propagation in PbBi was observed.
5. For Manet-II the different fracture mechanisms in air and PbBi were confirmed by microstructure investigations. In PbBi the formation of the first small crack resulted in fast crack propagation up to failure, in air many small surface cracks were observed.

Acknowledgements

The authors acknowledge E. Groth for the ingenious design of the PbBi container and for performing the fatigue tests.

References

[1] G.S. Bauer, J. Phys. IV France 9 (1999) 91.
[2] L.K. Mansur, H. Ullmaier, Proceedings of the International Workshop on Spallation Materials Technology, Oak Ridge National Laboratory Report CONF-9604151, 1996.
[3] J.P. Strizak, J.R. DiStefano, P.K. Liaw, H. Tian, J. Nucl. Mater. 296 (2001) 225.
[4] R.W. Swindeman, in: H.D. Solomon, G.R. Halford, L.R. Kaisand, B.N. Leis (Eds.), Low Cycle Fatigue, ASTM STP 942, American Society for Testing and Materials, Philadelphia, 1988, p. 107.
[5] Y. Asada, K. Dozaki, M. Ueta, M. Ichimiya, K. Mori, K. Taguchi, M. Kitagawa, T. Nishida, T. Sakon, M. Sukekawa, J. Nucl. Eng. Des. 139 (1993) 269.
[6] K. Natesan, O.K. Chopra, T.S. Kassner, Proceedings of the Second International Conference on Liquid Metal Technology in Energy Production, Richland, USA, 1980.